

Interactions in an Intensive Care Unit: Experiences Pre-Processing Sensor Network Data

Mauricio Monsalve
Department of Computer
Science
The University of Iowa
Iowa City, IA 52242
mauricio-monsalve
@uiowa.edu

Sriram Pemmaraju
Department of Computer
Science
The University of Iowa
Iowa City, IA 52242
sriram-pemmaraju
@uiowa.edu

Philip M. Polgreen
Department of Internal
Medicine
The University of Iowa
Iowa City, IA 52242
philip-polgreen
@uiowa.edu

ABSTRACT

Healthcare-associated infections (HAIs) represent a significant burden to healthcare provision; in the United States alone, it is estimated that approximately 2 million patients acquire HAIs each year. As part of a larger effort to understand how HAIs spread, we deployed a wireless sensor network in the Medical Intensive Care Unit of the University of Iowa Hospitals and Clinics. We used data reported by the network to estimate healthcare worker movement, interactions between healthcare workers, and adherence to hand sanitization policies.

Our experiment joins the growing yet still small collection of sensor network deployments in healthcare settings. This work contributes to this body of research by presenting a comprehensive approach to pre-processing the collected sensor data, thereby reducing errors and increasing robustness. We provide two main contributions: (i) a simple and theoretically sound calibration method for sensor signals that eliminates biases in pairwise sensor communication and (ii) filters that increase the reliability of signal strength from stationary sensors. We validate our methods by comparing visits of healthcare workers to rooms, as discovered from the sensor data, to ground truth room occupancy data collected in notes.

Categories and Subject Descriptors

J.3 [Computer applications]: Life and medical sciences—Health

General Terms

Experimentation, Measurement

Keywords

Sensor network, calibration, social sensing

Permission to make digital or hard copies of all or part of this work for personal or classroom use is granted without fee provided that copies are not made or distributed for profit or commercial advantage and that copies bear this notice and the full citation on the first page. To copy otherwise, to republish, to post on servers or to redistribute to lists, requires prior specific permission and/or a fee.

Wireless Health '13 Nov 1-3, 2013, Baltimore, MD, USA
Copyright 2013 ACM 978-1-4503-2290-4/13/11 ...\$15.00.

1. INTRODUCTION

Every year in the United States, healthcare-associated infections (HAIs) affect approximately 2 million patients, leading to approximately 100,000 deaths and generating a cost of 5 to 45 billion dollars according to different estimations [6, 18, 17]. This burden is intensified by the increasing appearance of antimicrobial-resistant infections [16]. It is well known that healthcare workers are an essential vector for the spread of HAIs [2, 20]. Frequent hand sanitization is seen as one of the most effective ways of preventing the spread of HAIs, and several guidelines specifying when and how hand sanitization must be performed have been developed [19, 2, 20]. These guidelines state, in general terms, that sanitization must occur before and after interacting with the patient and her environment, moments known as *opportunities for hand hygiene*. However, there is evidence to indicate that the rate at which healthcare workers satisfy these *opportunities* is generally below 50% [2, 20], which is considered insufficient to prevent the spread of HAIs.

A primary focus of the *Computational Epidemiology Research Group (compepi)* (<http://compepi.cs.uiowa.edu/>) at The University of Iowa is to understand the spread of HAIs at the University of Iowa Hospitals and Clinics (UIHC). Through most of the 20th century, compartmental disease-spread models such as SIR (Susceptible-Infected-Recovered) and its extensions [8] have provided analytical and computational tools for understanding the dynamics of disease spread in a relatively homogeneous population. With the availability of relatively cheap mobile technology that can report location, movement, etc., research in computational epidemiology has started to move away from the assumption that the underlying population is homogeneous and has instead started to rely on fine-grained data on individual location and movement. As part of a larger effort to understand the spread of HAIs at the UIHC, the compepi group deployed a wireless sensor network in the 20-bed Medical Intensive Care Unit (MICU) of the UIHC from June 1 to June 10, 2011. The goal was to measure both the interactions between healthcare workers and hand hygiene adherence. We continuously measured healthcare worker location information as well as their proximity with respect to each other, and recorded soap dispenser usage. The recorded data enables an understanding of contact patterns within the MICU, interactions between healthcare workers and patients, hand hygiene adherence, and how the proximity to other workers affects this adherence. This experiment is a follow-up of a

previous, similar deployment by the compepi group in the same unit [9].

Before the collected data can be used for the purposes stated above, it needs to undergo substantial pre-processing due to a number of problems with the sensor network technology and constraints on the deployment of the network. For example, even though the sensor motes had identical specifications, we detected consistent biases in pairwise communication between certain pairs of motes, e.g., mote A would consistently perceive a higher signal strength than mote B whenever motes A and B communicated with each other. Another problem was significant: rapid fluctuation in received signal strength, most likely caused by human movement, temporarily blocked signals.

In this work, we present a systematic approach for pre-processing the data collected through such a wireless sensor network experiment. We have two main contributions. First, we propose a simple and theoretically sound algorithm for calibrating signal strength readings in the context of reciprocal communication so as to remove biases in pairwise communication, which eliminates the need of carefully calibrating sensors individually. This method saves deployment time and uses all the data collected in the experiment. Second, we introduce several filters aimed at reducing signal fluctuations while keeping signal strengths reliable. These filters have to balance ignoring low signal strength values, which might have been caused by signal blockages, against paying close attention to low signal strength values that might indicate that the healthcare worker has moved away. We also propose mechanisms to deal with other problems in the data caused by clock drifts. Our pre-processing is aimed at reducing false positive and false negatives associated with the identification of events such as the visit by a healthcare worker to a room and the use of a soap dispenser by a healthcare worker. We conclude by presenting a simple verification for our pre-processing approach in which we show that rooms that are known to be empty at the beginning of a shift can be easily identified as being so by the sensor network data.

1.1 Related Work

Our experiment joins an increasing collection of wireless sensor network deployments in healthcare settings for measuring contact networks [9, 4, 12, 10] and electronic monitoring of hand hygiene adherence [13, 14]. But the number of experiments conducted so far is small and, thus, sharing experience is valuable. On the challenges posed by the deployments, Kazandjieva et al reported difficulties associated to sensor malfunction due to human factors, and ordered the recorded data by time using reference orders instead of clock synchronization [11]. Cattuto et al deployed a network of sensors that could not transmit further than 1-1.5 meters, which limited and simplified data processing [1, 10]. Frigery et al deployed a sensor network more similar to ours and detailed their data processing challenges in detail [4, 12]. Their main challenge arose from the unreliability of signal strengths to measure distance because signals attenuate with distance as well as with obstacles. Their visit detection method is similar to ours, the main difference being in that they use a single threshold while we apply a filter before testing thresholds, to minimize the effect of blocked signals on raw RSSI readings.

2. DEPLOYMENT DETAILS

2.1 Instrumentation

The objective of the experiment was to continuously record interpersonal contacts between healthcare workers in the MICU, which rooms were visited in the unit, and the workers' behavior with respect to hand washing. We did this through the deployment of a wireless sensor network that monitored the distance among workers and between workers and key physical locations, while also registering soap dispenser usage. We embedded Crossbow Telos Rev.B sensor modules [15] in wearable sensors or *badges* and stationary sensors or *beacons*. Figure 1 shows a Crossbow Telos Rev.B sensor module with an added battery and USB interface, and some sensor nodes. Badges were housed in recycled pagers, so healthcare workers could carry them on pockets at hip level. Beacons included *pyramids*, *bedmotes* and instrumented *soap dispensers*. Pyramids and bedmotes were to stay in a fixed location, typically on top of furniture and wall ledges, so their shape was designed to maximize stability. Instrumented soap dispensers consisted of recycled soap dispensers embedded with a sensor module that was activated upon usage.

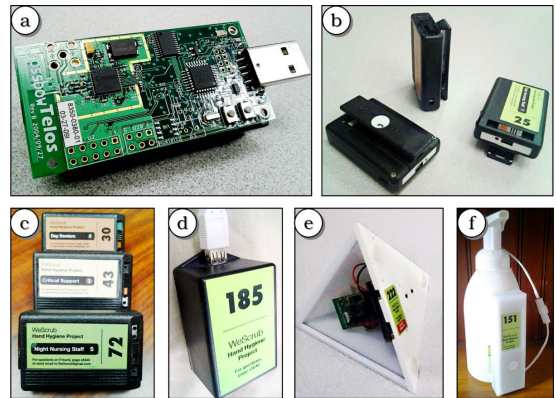


Figure 1: Sensors used in the experiment: (a) Crossbow Telos Rev.B, (b) wearable sensors or *badges*, (c) badges labelled by job type, (d) *bedmote*, (e) *pyramid*, (f) *instrumented soap dispenser*.

Proximity was sensed through the *Received Signal Strength Index* or RSSI; Crossbow Telos Rev.B sensor modules have an IEEE 802.15.4-compliant radio, meaning that all communication was performed through packets and that those packets always had a RSSI value associated to them [15]. The RSSI is a measure of the amount of power transmitted during communication. In Crossbow Telos Rev.B modules, this measure is linearly related to the logarithm of the transmitted power, and thus, to the logarithm of the distance between the antennas in absence of obstacles (refer to Chapter 1 of [5]). The antennas exhibit little differences in gain with angles. However, obstacles, such as the human body, can greatly absorb signal strength.

Throughout this article, we report RSSI values as we used them. RSSI are reported in different scales by different hardware, and are largely dependent on the architecture (layout, materials), obstacles, power settings, the structures housing the sensors, etc., making them unique per deployment. Telos Rev.B report RSSI in dBm, which we made positive by

adding 60 and discarded negative values as too insignificant. Beacons had an output power of 0 dBm while badges had an output power of -7 dBm, approximately.

We programmed the network in an asymmetric fashion. While badges, pyramids and bedmotes frequently sent packets informing their surrounding sensor nodes about their proximity, only badges recorded data. We also limited soap dispensers only to send data, which occurred only upon activation. When activated, soap dispensers would send three packets consecutively to guarantee reception.

The frequency at which badges, pyramids and bedmotes sent packets was identical. Packets would be sent every 7-12 seconds with randomization introduced to minimize packet collision and subsequent loss. The frequency was tuned to save battery life and reduce the amount of data recorded. In a similar way, clock synchronization occurred infrequently and through simple computation: badges would inform their time-stamp to their surrounding badges, which they would assume only if it was ahead of their own clock.

2.2 Execution

Sensors were placed in the unit according to their purpose: bedmotes were placed inside bedrooms (on a beam above patient beds), pyramids were placed outside bedrooms, in corridors and on top of furniture, and soap dispensers were placed outside and inside bedrooms. Figure 2 shows the floorplan of the MICU and the placement of the sensor nodes for the experiment.



Figure 2: Placement of the stationary sensors or beacons in the Medical Intensive Care Unit.

Once the unit was instrumented, two researchers wore several badges and walked around the unit with the purpose of collecting ground truth location information. In particular, they went to the door of each bedroom, standing still for about one minute per room, without going farther inside. This process gave us "ground truth" RSSI values for communication between bedmotes and badges at the door of corresponding rooms.

The experiment was conducted after this setup. Between shifts (at 6 am and at 6 pm), a researcher would collect and distribute badges to the healthcare workers according to their job type. We did not record any additional information about workers to respect their anonymity. We distinguished six job types: day doctors, day nurses, day critical care personnel, night doctors, night nurses and night critical care personnel. Each badge's data was copied and erased each time the badge was collected.

A computer server was set up to monitor the *health* of the sensor nodes. This functioned as follows: a probe would be

sent to the network asking a reply for every sensor node. If a node did not reply, it was examined and possibly replaced. Soap dispensers required periodical attention because their pumps would stop working or they would run out of soap.

2.3 Collected data

Upon completion of the experiment, we had collected data of 10 day and 9 night shifts. We merged all the data corresponding to each shift in single files structured as:

receiver	time	sender	rsssi
...
77	2011-06-09:20:22:05	31	20
82	2011-06-09:20:22:05	79	17
78	2011-06-09:20:22:06	192	20
31	2011-06-09:20:22:06	195	25
...

Each line corresponds to a packet received by a badge. The **time** field contains the time-stamp according to the badge receiving the packet. The **receiver** field contains the id number of the badge receiving the packet. The **sender** field contains the id number of the badge sending the packet. Finally, the **rsssi** field contains the RSSI value associated to the reading. Each file was sorted according to the time field.

Packet loss was predominant when sensors were distant. For instance, for $RSSI = 15$, packet loss was about 50% (average over windows of 1 minute). Packet loss, however, decreased dramatically as RSSI values rose, being around 10% for $RSSI = 30$ and below 3% for $RSSI \geq 40$.

2.4 Data processing challenges

Our main objective was to identify two types of events: (i) *visit identification*: when a worker visited a room; and (ii) *hand hygiene identification*: when a worker used a soap dispenser. We are also interested in when pairs of workers are within some range of each other. However, before we can do any of these tasks, we needed to remove artifacts in the data that were due to unreliability of sensors or blockages of signals.

When inspecting the collected RSSI values, we found that they were subject to strong *fluctuations*. Ideally these fluctuations would have been due to movement of workers, but that was not the case. Figure 3 shows some fluctuations in received RSSIs between a badge and a bedmote. The worker went inside the bedroom between minutes 2 and 3; we know so because $RSSI \geq 45$ implies that the worker was inside the room for this pair of sensors. We also see that the RSSI alternated between being greater than 45 and smaller than 45 approximately every 8 seconds. It is unlikely that the worker entered and left the room at such frequency. We conjecture that RSSI fluctuations must have been caused by signals being blocked, besides movement.

One could suggest using a moving average RSSI filter to reduce the variability of the RSSI values. However, flat averages are misleading; the average RSSI between minutes 2 and 3 is roughly the same as in minute 16, yet the worker was outside the room in the later. (Figure 3 depicts a moving average consisting of 5 observations.) Instead, we must notice that not all RSSI values are as reliable. Since attenuation can be caused by blocked signals, higher values are more reliable than smaller ones, and smaller values are specially unreliable when surrounded by greater ones. We must design a filter that discriminates between RSSI values. The application of such filter is visit detection. Proximity

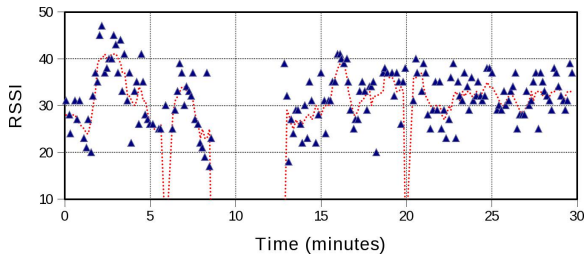


Figure 3: RSSI fluctuations in the communication between two sensors: badge 1 and bedmote 188. The blue triangles represent the raw RSSI values while the dotted red line represents their moving average.

between workers is always changing and fluctuations can be well explained by movement in such case.

We also observed that the RSSI reported by badges in reciprocal communication was sometimes systematically biased: one sensor could read RSSI values systematically higher than its counterpart. Figure 4 illustrates one such situation. This should not be physically possible if the sensors were exactly identical. It is thus necessary to remove such biases to ensure the signal strengths they report share the same scale.

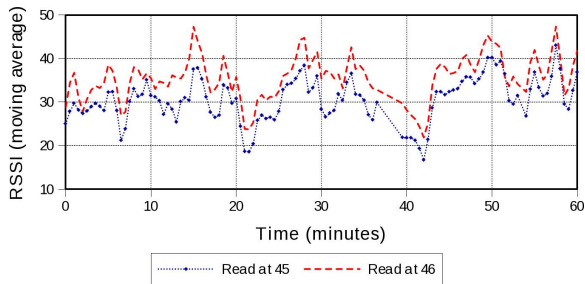


Figure 4: Example of systematically biased communication between two sensors: badges 45 and 46.

3. SENSOR CALIBRATION

3.1 Badge-to-badge asymmetries

Further analysis of the biases between RSSI values in reciprocal communication shows that reciprocal readings follow a linear dependence. Figure 5 illustrates three pairs of badges that are unbiased towards each other and it also illustrates three pairs of badges that are biased toward each other. Each point in these plots represents a 30 second window in which both sensors read 3 or 4 messages from their counterparts. The RSSI values assigned to each window correspond to the arithmetic averages of the readings at each sensor.

These asymmetries imply that not all sensors perceive the RSSI in the same scale. From Fig. 5, we see that what is $RSSI = 50$ for badge 45 roughly corresponds to $RSSI = 60$ for badge 46. (Later we show that RSSI of these magnitudes are very important in the analysis.) Therefore, we needed to unify the RSSI in the same scale.

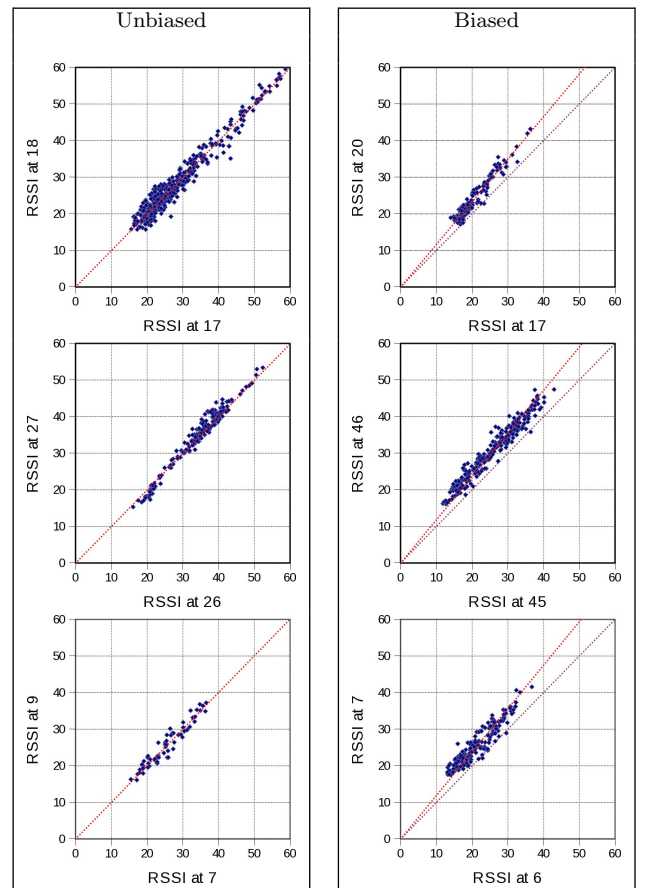


Figure 5: RSSI in reciprocal communication. The three plots to the left depict nearly symmetrical readings. The three plots to the right depict asymmetrical readings. The dotted red line illustrates the bias (inclination) of the reciprocal readings and the dotted purple line illustrates the identity line (in the biased plots).

3.2 Calibration model

We now introduce the model we used to calibrate the RSSI values read by the sensors. Let us imagine that the RSSI values are continuously known and define $x_{AB}^A(t)$ as the RSSI sensed by badge A at time t , in the communication between A and B . We can then write the following equation that relates the mutual readings of two sensors:

$$x_{AB}^A(t) = a_{AB}x_{AB}^B(t) + b_{AB},$$

where a_{AB} and b_{AB} are constants. This linear affine relation is inspired by the relations observed in the data (as in Fig. 5). We have omitted error terms because this is not a statistical model but an ideal one. However, if we were to fit this model, we would use an additive normal error with mean zero.

We cannot make use of the above model to calibrate the sensors because it does not explicitly make use of a unique scale. All of its constants are defined between pairs of sensors. So, let us suppose that there exist ideal sensors with a unique scale, and define $x_{AB}(t)$ as the unbiased RSSI received by both A and B . Since they share the same scale, $x_{AB}(t) = x_{BA}(t)$. We can then write the following relation

between the RSSI of a biased sensor and the RSSI of an idealized unbiased sensor:

$$x_{AB}^A(t) = a'_{AB}x_{AB}(t) + b'_{AB},$$

where a'_{AB} and b'_{AB} are constants.

Let us attribute causes to the above terms. We assume that bias can occur in the communication between antennas due to differences in gain and power output. Since Telos Rev.B modules report signal strength in a logarithmic scale (its RSSI is a linear transformation of the Received Signal Strength, measured in dBm), both the *volume* (gain and power at the sender) and the *sensitivity* (gain at the receiver) biases are additive to the unbiased signal $x_{AB}(t)$. (Since the transmitted power is $\mathcal{E} \propto g_A g_B d(t)^{-k}$, where g_A and g_B are the gains, $d(t)$ is the distance, and $k > 0$ is the signal attenuation constant, then $x_{AB}(t) = \log_{10} g_A + \log_{10} g_B - k \log_{10} d(t) + \epsilon$. Refer to Chapter 1 of [5] for antenna theory.) Bias can also occur in the conversion of analog signals, which are continuous, to digital signals, which are discrete. We can attribute the inclination a'_{AB} to this source of bias, as well to an additional constant term in the readings.

Considering the above relations between the constants and the sensors, we assume the following calibration model:

$$x_{AB}^A(t) = s_A (x_{AB}(t) + v_B) + c_A,$$

where s_A is the proportional scale bias of badge A (an electronic bias), v_B is the volume of badge B , and c_A are the additive biases at badge A , which include its antenna sensitivity and electronic bias. The error terms are introduced when we take into account that we only have a spare sample of the RSSI values.

Upon performing linear regression to the mutual RSSI readings (e.g. as in Fig. 5), we observed that the constant terms were often very small or that, if ignored, we could still fit the curves quite well (R^2 reductions in the second or third decimal places). Thus, we decided to ignore the constant biases, obtaining the simpler model:

$$x_{AB}^A(t) \approx s_A x_{AB}(t).$$

This model implies that the proportionality bias ends up making the additive biases unimportant. This is probably a consequence of the high RSSI readings obtained when the badges were in close proximity, and might not apply for scenarios where sensors must sense neighbors that are distant.

3.3 Badge-to-badge calibration algorithm

If the previous model were to be approximately correct, then we could estimate s_A/s_B by computing the ratio $\alpha_{AB} = \langle x_{AB}^A(t) \rangle / \langle x_{AB}^B(t) \rangle$. In situations where sensors do not directly communicate with each other we use transitivity to estimate this ratio. More specifically, suppose that badges A and C did not communicate directly with each other. Then, we could estimate s_A/s_C through *transitivity*:

$$\frac{s_A}{s_C} = \frac{s_A s_B}{s_B s_C} \Rightarrow \alpha_{AC} \approx \alpha_{AB} \alpha_{BC},$$

an estimation which can be improved by taking the average over all intermediate badges B :

$$\tilde{\alpha}_{AC} = \frac{1}{n} \sum_B \alpha_{AB} \alpha_{BC},$$

where n is the number of intermediate badges B .

Estimation of the ratios α_{AB} through $\tilde{\alpha}_{AB}$ allows us to estimate missing ratios that we cannot compute directly from the data. Our calibration procedure requires knowing all the ratios α_{AB} . Thus, the quality of the estimation $\tilde{\alpha}_{AB}$ is relevant, and we assessed it through experimentation. For day shift 8, we computed all ratios α_{AB} and then estimated them using $\tilde{\alpha}_{AB}$. Figure 6 shows the results for day shift 8. Points far from the cloud correspond to ratios estimated using few observations. The estimation becomes tight when the other shifts are considered as well.

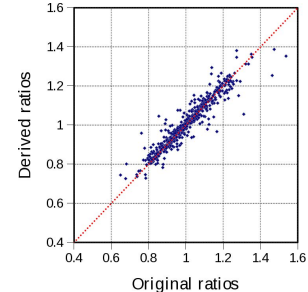


Figure 6: Testing the transitivity of edge-ratios in day shift 8. The x-axis depicts the derived ratio $\tilde{\alpha}_{AB}$ while the y-axis depicts the actual ratio α_{AB} , for all pairs of badges A and B that communicated.

The following calibration algorithm is an immediate consequence of this empirical property. First, compute all ratios $\alpha_{AB} = \langle x_{AB}^A(t) \rangle / \langle x_{AB}^B(t) \rangle$. Then, for all pairs A, B such that α_{AB} is missing, estimate α_{AB} through $\tilde{\alpha}_{AB}$. Once every α_{AB} is computed, proceed to compute constants $\alpha_A = \frac{1}{n} \sum_B \alpha_{AB}$, n being the number of badges. Then, replace the RSSI values $x_{AB}^A(t)$ by $x_{AB}^A(t)/\alpha_A$. All the RSSI will be in the same scale.

The rationale behind the above is very simple. If $\alpha_{AB} = s_A/s_B$, then $\alpha_A = \frac{1}{n} s_A \sum_B s_B^{-1}$. Thus, $\alpha_A = \alpha s_A$, $\alpha_B = \alpha s_B$, etc. for $\alpha = \frac{1}{n} \sum_A s_A^{-1}$. Then, we have that $x_{AB}^A(t)/s_A = x_{AB}(t)/\alpha$. Since all readings become proportional to the ideal readings through the same scaling factor α^{-1} , all the readings are in the same scale. (We could have chosen $\alpha_A = \sum_B \alpha_{AB}$ instead of $\alpha_A = \frac{1}{n} \sum_B \alpha_{AB}$, but we did not want to modify $x_{AB}^A(t)$ that much.)

3.4 Bed-to-badge calibration

Having calibrated badges, we proceeded to calibrate bedmotes. Our objective here was to ensure that all the RSSI of the bedmotes to their corresponding doors (R_{DOOR}) was the same. Differences in R_{DOOR} was mainly the consequence of differences in the distance between the doors and the beds, which is where the bedmotes were located. These differences were partially induced by the shape of the rooms (see Fig. 2) and the orientation and location of beds with respect to doors.

Measurement of R_{DOOR} was performed in the walk-through. Recall that researchers stood still in each door for about one minute, and did not go farther inside the rooms during the tour. The highest RSSI readings, then, correspond to R_{DOOR} . We took the 10 highest RSSI readings from each bedmote, and computed the respective averages to compute each R_{DOOR} . Ten signals correspond, roughly, to 80 seconds, and the average served as a stable measure of R_{DOOR} .

Calibration was performed to ensure that $R_{DOOR} = \langle R_{DOOR} \rangle$ for all bedmotes; this value corresponds to the average of the previous values. Let $R_{DOOR}^{bedmote}$ be the R_{DOOR} corresponding to a given bedmote. We used the following formula to re-scale the RSSI values to the bedmotes:

$$RSSI_{calibrated}^{bedmote} = RSSI_{raw}^{bedmote} \frac{\langle R_{DOOR} \rangle}{R_{DOOR}^{bedmote}}.$$

We obtained $\langle R_{DOOR} \rangle \approx 51.08$.

4. FILTERS FOR SIGNAL STRENGTH

4.1 Filtering soap dispenser usage

An essential part of our experiment consisted of measuring hand sanitization. This required identifying when a soap dispenser was activated and which badge was the closest to it. Since soap dispensers sent three packets upon activation and these packets may have been received by all the surrounding badges, soap dispenser usage was recorded with considerable replication. In addition to this amount of replication, packets appeared to have echo in the data, consequence of the inaccuracies of the clocks embedded within the badges. Figure 7 shows an event overheard by 7 badges during a period of 6 seconds. Our objective is to identify the *true events* of soap dispenser usage.

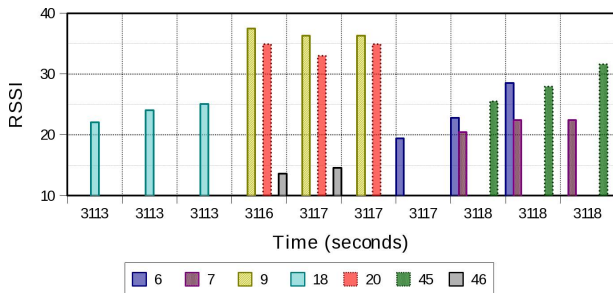


Figure 7: Replication of a soap dispenser usage event. Bars of different styles represent readings by different badges.

After examining the messages sent by the soap dispensers, we found that nearly all of them occurred within a 10 second interval. In that interval, the event was most likely triggered by the worker wearing the badge that received the highest RSSI. Given the quick fluctuations in RSSI values, we cannot be completely sure that that was the right badge, but it is our best estimate.

Some situations can trigger false positives (wrongly attributed activation events). For example, when two badges are identically close to the soap dispenser when it is activated. In this case, the sanitization event may be attributed to the wrong badge, but it is unlikely that a person in this situation is not incurring or has not incurred an opportunity, so it does not affect the final statistics.

False positives can be also produced by a person activating a soap dispenser but not wearing a badge. In this case, the maximum signal strength perceived among the surrounding badges would not be as large as when a worker wearing a badge activated the dispenser. Unfortunately, given the large variability of the signal strengths, we cannot completely rule out these cases. Still, we found a distortion in

the probability distribution of the dispenser usage readings: the RSSI encountered a minimum. We discard this distortion by asking that highest RSSI to be greater than 36.

False negatives (missed events) occurred when workers washed their hands in quick succession using the same dispenser. These situations can be detected by observing the density of messages read during a time window. Fortunately, they seemed to be very rare.

4.2 Filtering RSSI from beacons

The objective of applying filters to proximity-related RSSI values is two-fold. First, we would like to have continuous estimates of RSSI values in time. For example, if we have two successive RSSI of 40 and then 55, we would like to know when the RSSI crossed 50. And second, we would also like to reduce the variability in the data and make the RSSI a better proxy for distance.

As we have discussed, signal strength attenuates with both distance and obstacles, such as the human body. We would like to reduce the effect of obstacles as much as possible. So far, we can only identify blocked signals when they are surrounded by high signals. In general, we would like to ignore quick reductions in signal strength. At the same time, high RSSI values are more reliable than the rest, because they can only occur in close proximity.

Our approach consists in estimating $x_{AB}(t)$ through a weighted moving average of RSSI observations. We consider observations within a time window of 60 seconds around time t , i.e. in the interval $[t - 30, t + 30]$. We prioritize observations according to their proximity in time to t and according to their *relative magnitude* with respect to the surrounding observations.

Let x_τ be an observation (RSSI) taken at time τ and let $S(t) = \{x_\tau : t - 30 \leq \tau \leq t + 30\}$ be the set of observations associated to the time window $[t - 30, t + 30]$. Now, let us define the *temporal weights* $\omega_T(\Delta t)$ as:

$$\omega_T(\Delta t) = \frac{1}{a + \Delta t^2},$$

where a is a tuning constant. From this definition, we proceed to define the moving average filter $\mathcal{A}(t)$ as:

$$\mathcal{A}(t) = \frac{\sum_{x_\tau \in S(t)} x_\tau \omega_T(t - \tau)}{\sum_{x_\tau \in S(t)} \omega_T(t - \tau)}.$$

Filter $\mathcal{A}(t)$ defines the *local magnitude* of the set of observations $S(t)$.

The temporal weights $\omega_T(\Delta t)$ configures how much an observation weights when it is Δt time away from time t . We chose a so that an observation 15 seconds away from t weights 50% of an observation at time t ; thus, we chose $a = 15^2$.

Having defined the local magnitude, we define the relative magnitude of x_τ as the difference between x_τ and $\mathcal{A}(t)$: $\Delta x_\tau(t) = x_\tau - \mathcal{A}(t)$. This definition depends on both τ and t , so an observation x_τ has a different relative magnitude according to the different time window in which is used.

Now, let us give priority to observations according to their difference with respect to the local magnitude. Let us define the *magnitude weight* $\omega_M(x, t)$ as:

$$\omega_M(x, t) = b + \max(0, x - \mathcal{A}(t)).$$

An observation below the local magnitude $\mathcal{A}(t)$ will receive a minimum weight b . We have chosen $b = 4^2$ because fil-

ter $\mathcal{A}(t)$ is very local, and any deviation from it appears significant.

We now introduce the full formula of our *priority* filter $\mathcal{P}(t)$. For this filter, we use both the temporal and magnitude weights, and replace observations below the local magnitude $\mathcal{A}(t)$ with the local magnitude. We define $\mathcal{P}(t)$ as:

$$\mathcal{P}(t) = \frac{\sum_{x_\tau \in S(t)} \max(x_\tau, \mathcal{A}(t)) \omega_T(t - \tau) \omega_M(x_\tau, t)}{\sum_{x_\tau \in S(t)} \omega_T(t - \tau) \omega_M(x_\tau, t)}.$$

Note that, if constant b of ω_M is adjusted accordingly, this filter is commutative with increasing linear transformation applications on x_τ . Thus, our calibration methods work both before or after application of this filter.

This filter has a strong weakness: it fails to provide reasonable estimation in the presence of strong packet loss. This can be fixed, however, by introducing *false zero observations* to set $S(t)$. Using the modified $S'(t) = S(t) \cup \{\hat{x}_{t-30} = 10, \hat{x}_{t+30} = 10\}$ instead of $S(t)$ should suffice. This way, the false observations will have an effect when there are few readings in the interval $[t - 30, t + 30]$.

Figure 8 illustrates the effect of filters $\mathcal{A}(t)$ and $\mathcal{P}(t)$ on the data. As we can see, the priority filter $\mathcal{P}(t)$ follows the locally maximum RSSI closely.

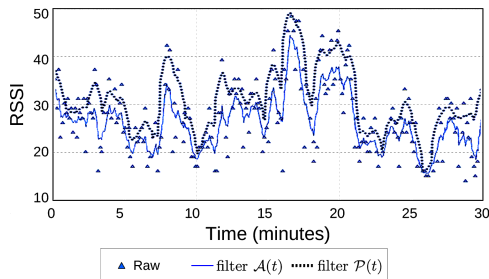


Figure 8: Comparison of different filters for continuous RSSI data.

5. INTERPRETING THE DATA

5.1 Identifying visits and measuring adherence

In principle, we wanted to test two conditions for detecting whether a worker visited a room: that the RSSI to the room was the highest, and that that RSSI was greater than the RSSI value at the door. But we needed to relax these conditions, because the signal strengths we obtained were not as steady as in the walk through the unit. Instead, workers often walked in front of each other, blocking the signals, they were moving in all directions, etc, which made RSSI unstable and different from the cleaner readings obtained in the walk-through.

Robust visit identification required relaxing the previous conditions. We relaxed the second condition, which required the RSSI to be above $R_{DOOR} \approx 51$ during the whole visit. The condition about the closest bedmote being the closest during the whole visit could not be relaxed, as it would truly mean that another bedmote was closer.

We identified visits as follows. We tested whether the highest RSSI to a bedmote was above 49 (instead of 51). If so, the person was considered to be visiting that room. If the closest bedmote changed or the highest RSSI fell below 43, then the visit is terminated. ($RSSI = 43$ may appear

to be much smaller than $RSSI = 49$, but a difference of 6 units is small in comparison to the variability of RSSI.)

In addition, a visit is discarded if the maximum RSSI to the bedmote did not exceed a threshold. This threshold can be tuned to discard false positives; a value above 51 should ensure that the worker actually went farther inside the room. We use a value of 52.5 in the next subsections.

Now, there are two moments that are important in a visit: room entry and room exit. Both represent opportunities for hand hygiene, which shall be complied by the corresponding worker by using a soap dispenser. We defined the room entry time as the first time the RSSI to the bedroom was above 49. Analogously, we defined the room exit time as the last moment that RSSI was above 49.

The above values have been chosen heuristically, to approximate the identification of visits in an ideal scenario. These settings nearly minimize the identification of false visits. Further relaxation of these settings would reveal more visits while introducing errors.

5.2 Testing visits on empty rooms

To validate that our method for detecting visits, we tested it against ground truth data. As mentioned, notes were taken between shifts, while badges were collected and handed out again. Which rooms were empty or labeled as *special precautions* were among the items recorded in those notes. This means that we know which rooms were empty and which were occupied at the beginning and end of each shift without depending on the sensor data. Therefore, we can test whether an empty room was less likely to be visited than an occupied room. At the beginning of each shift, visits to empty rooms should be unlikely. However, as each shift progresses, visits to empty rooms should become likely as the rooms became occupied. But our notes report that some rooms remained empty across shifts; visits to those rooms should remain unlikely throughout entire shifts.

For each shift, we divided rooms into three categories: *continuously empty rooms*, which were empty at the start and at the end of the shift; *non continuously empty rooms*, which were empty only at the beginning; and *occupied rooms*, which were occupied at the beginning. We then proceeded to compute the average number of visits each room received since the start of the shift until its first, fourth and eighth hour, per type of room. We expect the frequency of visits to be significantly different across room types. Continuously empty rooms should receive significantly less visits than other rooms throughout the shift. Non continuously empty rooms should receive increasingly more visits throughout the shift, as these rooms become occupied by incoming patients. Occupied rooms should receive the highest number of visits throughout the day, in spite that, by the eighth hour, the frequency of visits should decrease as their occupying patients are discharged. In particular, we expect the frequency of visits to non continuously empty and occupied rooms to become similar to the eighth hour; we expect that patient arrival and discharge rates were similar during the experiment. (Otherwise the unit would have had reached maximum occupancy.)

Figure 9 illustrates the measures along with their 95% confidence intervals. Disjoint confidence intervals demonstrate that the measures are significantly different in statistical terms [3]. The differences between the measures are also significantly different in terms of magnitude. Continuously

visited rooms received considerably less visits than the other two types of rooms. Non continuously visited rooms received an increasing number of visits, as expected. Occupied rooms received considerable more visits than the previous rooms. And to the eighth hour, we observe that non continuously empty and occupied rooms received a similar number of visits, as expected. We consider that the measures are realistic and satisfy our expectations.

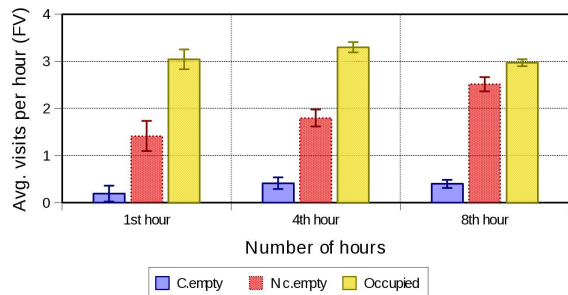


Figure 9: Average number of visits per hour and per room, by room type: continuously empty rooms (*C.empty*), non continuously empty rooms (*Nc.empty*), and occupied rooms (*Occupied*).

6. CONCLUSIONS

This paper presents a systematic approach to pre-processing wireless sensor network data in order to make it more robust. The sensor network data in this paper is obtained from a deployment in an intensive care unit in a hospital. However, the approach should work for sensor data obtained in other settings as well. After completing the pre-processing step described in the paper, we have begun to use the sensor network data for two purposes. We have used the sensor data to identify proximity between healthcare workers and used this to construct healthcare worker *contact networks* with the intensive care unit [7]. We have also started to use this data to correlate hand hygiene adherence to the presence of peers nearby, thus identifying the effect of peers on hand hygiene adherence.

7. REFERENCES

- [1] C. Cattuto, W. Van den Broeck, A. Barrat, V. Colizza, J.-F. Pinton, and A. Vespignani. Dynamics of person-to-person interactions from distributed RFID sensor networks. *PloS one*, 5(7):e11596, Jan. 2010.
- [2] Centers for Disease Control and Prevention. Guidelines for Hand Hygiene in Healthcare Settings. *Morbidity and Mortality Weekly Report*, 51(Oct 25):RR-16, 2002.
- [3] J.-B. du Prel, G. Hommel, B. Röhrig, and M. Blettner. Confidence interval or p-value?: part 4 of a series on evaluation of scientific publications. *Deutsches Ärzteblatt international*, 106(19):335–9, May 2009.
- [4] A. Friggeri, G. Chelius, E. Fleury, A. Fraboulet, F. Mentré, and J. Lucet. Reconstructing social interactions using an unreliable wireless sensor network. *Computer Communications*, 34(5):609–618, Apr. 2011.
- [5] C. Haslett. *Essentials of Radio Wave Propagation*. Cambridge University Press, New York, New York, USA, 1st edition, 2008.
- [6] M. Hassan, H. P. Tuckman, R. H. Patrick, D. S. Kountz, and J. L. Kohn. Cost of hospital-acquired infection. *Hospital topics*, 88(3):82–9, 2010.
- [7] T. Herman, M. Monsalve, S. V. Pemmaraju, P. Polgreen, A. M. Segre, D. Sharma, and G. Thomas. Inferring realistic intra-hospital contact networks using link prediction and computer logins. In *SocialCom/PASSAT*, pages 572–578, 2012.
- [8] H. W. Hethcote. The mathematics of infectious diseases. *SIAM Review*, 42(4):599–653, 2000.
- [9] T. Hornbeck, D. Naylor, A. M. Segre, G. Thomas, T. Herman, and P. M. Polgreen. Using sensor networks to study the effect of peripatetic healthcare workers on the spread of hospital-associated infections. *The Journal of Infectious Diseases*, 206(10):1549–57, Nov. 2012.
- [10] L. Isella, M. Romano, A. Barrat, C. Cattuto, V. Colizza, W. Van den Broeck, F. Gesualdo, E. Pandolfi, L. Ravà, C. Rizzo, and A. E. Tozzi. Close encounters in a pediatric ward: measuring face-to-face proximity and mixing patterns with wearable sensors. *PloS one*, 6(2):e17144, Jan. 2011.
- [11] M. A. Kazandjieva, J. W. Lee, M. Salathé, M. W. Feldman, J. H. Jones, and P. Levis. Experiences in measuring a human contact network for epidemiology research. In *Proceedings of the 6th Workshop on Hot Topics in Embedded Networked Sensors - HotEmNets '10*, page 1, New York, New York, USA, 2010. ACM Press.
- [12] J.-C. Lucet, C. Laouenan, G. Chelius, N. Veziris, D. Lepelletier, A. Friggeri, D. Abiteboul, E. Bouvet, F. Mentre, and E. Fleury. Electronic sensors for assessing interactions between healthcare workers and patients under airborne precautions. *PloS one*, 7(5):e37893, Jan. 2012.
- [13] A. R. Marra, D. F. Moura, A. T. Paes, O. F. P. a. dos Santos, and M. B. Edmond. Measuring rates of hand hygiene adherence in the intensive care setting: a comparative study of direct observation, product usage, and electronic counting devices. *Infection Control and Hospital Epidemiology*, 31(8):796–801, Aug. 2010.
- [14] D. J. Morgan, L. Pineles, M. Shardell, A. Young, K. Ellingson, J. A. Jernigan, H. R. Day, K. A. Thom, A. D. Harris, and E. N. Perencevich. Automated hand hygiene count devices may better measure compliance than human observation. *American journal of Infection Control*, 40(10):955–9, Dec. 2012.
- [15] J. Polastre, R. Szewczyk, and D. Culler. Telos: enabling ultra-low power wireless research. In *IPSN 2005. Fourth International Symposium on Information Processing in Sensor Networks, 2005.*, pages 364–369. IEEE, 2005.
- [16] R. R. Roberts, B. Hota, I. Ahmad, R. D. Scott, S. D. Foster, F. Abbasi, S. Schabowski, L. M. Kampe, G. G. Ciavarella, M. Supino, J. Naples, R. Cordell, S. B. Levy, and R. A. Weinstein. Hospital and societal costs of antimicrobial-resistant infections in a Chicago teaching hospital: implications for antibiotic stewardship. *Clinical Infectious Diseases*, 49(8):1175–84, Oct. 2009.
- [17] R. R. Roberts, R. D. Scott, B. Hota, L. M. Kampe, F. Abbasi, S. Schabowski, I. Ahmad, G. G. Ciavarella, R. Cordell, S. L. Solomon, R. Hagtvedt, and R. A. Weinstein. Costs attributable to healthcare-acquired infection in hospitalized adults and a comparison of economic methods. *Medical care*, 48(11):1026–35, Nov. 2010.
- [18] R. D. I. Scott. The Direct Medical costs of and the Benefits of Prevention. *Hospitals*, (March):1–16, 2009.
- [19] B. Simmons, J. Bryant, K. Neiman, L. Spencer, and K. Arheart. The role of handwashing in prevention of endemic intensive care unit infections. *Infection Control and Hospital Epidemiology*, 11(11):589–94, Nov. 1990.
- [20] World Health Organization. WHO Guidelines on Hand Hygiene in healthcare. Technical report, 2009.